International Journal of Precision Engineering and Manufacturing (2019) 20:45–52
https://doi.org/10.1007/s12541-019-00039-7

Online ISSN 2005-4602
Print ISSN 2234-7593

REGULAR PAPER

Friction Drilling of Cast Aluminum Alloy A380 Without Significant Petal Formation and Radial Fracture

Sara Ahmed El-Bahloul[1]

Received: 24 June 2018 / Revised: 27 August 2018 / Accepted: 31 October 2018 / Published online: 7 February 2019

Abstract
Cast aluminum alloy A380 is one of the most commonly specified alloys that has light weight and exhibits excellent resistance to hot cracking, which makes it necessary in many industrial applications. An idea is investigated to generate a cylindrical bushing without significant petal formation and radial fracture that are expected to be obtained by friction drilling of cast metals. Three materials; namely, 316 stainless steel, Al6060 aluminum alloy, and red copper alloy are used in which each of them is located on the upper and lower surfaces of A380 workpiece, so achieving the idea of the functionally graded material. The process parameters were studied for reducing the resultant axial force, the gap between surfaces, and achieving a longer bushing without petal formation and radial fracture. Lower feed rate achieves minimum axial force and gap thickness with maximum bushing length for all material sandwiches. An optimized decision making by the help of fuzzy logic techniques is performed, revealing that red copper sandwich exhibits the optimal multiple performance characteristic index based on axial force, bushing length, gap thickness, and gap divergence.

Keywords Thermal friction drilling · Cast aluminum alloy · Axial force · Bushing length · Gap thickness · Gap divergence

List of Symbols

Np	Normalized axial force, bushing length, gap thickness, or gap divergence for every experiment number *p*
Xp	Axial force, bushing length, gap thickness, or gap divergence for an experiment number *p*
Xmax	Maximum value of the axial force, bushing length, gap thickness, or gap divergence for all experiment
Xmin	Minimum value of the axial force, bushing length, gap thickness, or gap divergence for all experiment

1 Introduction

A380 cast aluminum alloy is one of the most commonly specified aluminum alloys that offers the best combination of mechanical and thermal properties. It exhibits excellent fluidity, pressure tightness, and resistance to hot cracking. Also, it is used for a wide variety of products including chassis for electronic equipment, engine brackets, gearbox cases, household furniture, power, and hand tools [1].

Thermal friction drilling, also called friction stir drilling, form drilling, or flow drilling is a hole-making nonconventional method. The friction occurred between a rotating tool and a workpiece produces heat that softens the work material and allows tool penetration, leading to bushing formation as shown in Fig. 1. As the obtained bushing can be threaded and provides the more load-bearing surface of high strength, friction drilling can join sheet materials in a simple and economical way [2].

Miller et al. [3] investigated two ideas of pre-heating the workpiece or using high rotational speed for friction drilling of cast aluminum A380 and cast magnesium MgAZ91D alloys, in order to generate a free radial fracture or petal formation bushing. The shape and quality of A380 bushing were improved at higher workpiece temperature. For MgAZ91D alloy both preheating the workpiece or using high spindle speed at room temperature had a detrimental effect on the bushing shape. Lee et al. [4] friction drilled a nickel-based cast super-alloy IN-713LC under different feed rates and rotational speeds. Experimental results revealed that hardness was greater near the

✉ Sara Ahmed El-Bahloul
sara_elbahloul@mans.edu.eg

[1] Production and Mechanical Design Engineering Department, Faculty of Engineering, Mansoura University, Mansoura, Egypt

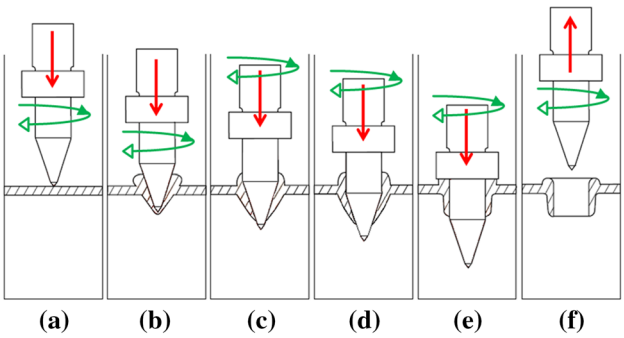

Fig. 1 Friction drilling steps: **a** initial contact; **b** tool-tip penetration to the material; **c** material flow; **d** tool-cylindrical region penetration; **e** bushing forming; **f** tool withdrawal

hole's wall. Moreover, higher rotational speed and faster feed rate yielded better roundness. Yang et al. [5] applied thermal friction drilling on three Ni-based super-alloys; Mar-M247, Haynes-230 and Inconel-718, using different spindle speed and feed rate to explore the bush length and internal hole of drilled surface roughness. The results showed that the longest bush length and best surface roughness were for Haynes-230; however, Inconel-718 had the largest axial force and worse bush length and surface roughness. Biermann and Liu [6] investigated flow drilling of magnesium wrought alloy AZ31, in which blind holes were machined in thin-walled profile. It was found that when feed rate increased, thrust force and torque increased. Kaya et al. [7] investigated the effects of different drilling parameters on workpiece surface temperature, thrust force, and torque in friction drilling of ST12 material. Experimental results revealed that the thrust force and torque increased with increasing friction angle, feed rate and friction contact area ratio, and decreasing drilling speed. Urbikain et al. [8] made a combination of friction drilling and form tapping processes on dissimilar materials for making nutless joints. The process parameters were studied for reducing the gap between surfaces and producing a good cup for making the posterior threading. The gap was decreased by increasing spindle speed and decreasing the feed rate and plate thickness.

This research investigates an idea to generate a cylindrical bushing without significant petal formation and radial fracture that is expected to be obtained by friction drilling of cast metals. Three materials; namely, 316 stainless steel, Al6060 aluminum alloy, and red copper alloy are used as a sheet metal of 1 mm thickness, in which each of them is located on the upper and lower surfaces of A380 workpiece of 5 mm thickness, achieving the idea of the functionally graded material. Table 1 illustrates the material properties of the A380 cast aluminum alloy, 316 stainless steel, Al6060 aluminum alloy, and red copper alloy. The process parameters are studied for reducing the axial force peak (AF), gap thickness (GT) and gap divergence (GD), and increasing the bushing length (BL), with achieving a good bushing without significant petal formation and radial fracture. When the AF is decreased, lower power consumption occurs, so lower machining cost. When longer BL is achieved, a more bearing area that can be threaded will be available. When the gap is minimized, less metal corrosion occurs.

Table 1 Material composition and properties of the A380 cast aluminum alloy, 316 stainless steel, Al6060 aluminum alloy, and red copper alloy

	Tensile stress (MPa)	Elastic modulus (GPa)	Elongation (%)	Density (kg/m^3)	Specific heat (J/kg K)	Thermal conductivity (W/m K)	Coefficient of thermal expansion (μm/m/°C)	Hardness (Brinell)
A380 cast aluminum alloy	324	71	3	2710	870	96.2	21.8	80
316 stainless steel	515	193	40	8000	500	16.3–21.5	15.9–17.5	212
Al6060 aluminum alloy	140–230	69.5	8	2700	900	209	23.4	60
Red copper alloy	394	118	12	8747	377	160	10.4	111

A380 cast aluminum alloy	Al	Cu	Mg	Fe	Pb	Ni	Zn	Mn	Si
	Bal.	3–4	0.1	1.3	0.35	0.5	3	0.5	7.5–9.5
316 stainless steel	C	Mn	Si	P	S	Cr	Mo	Ni	N
	0.08	2.0	0.75	0.045	0.03	16–18	2–3	10–14	0.1
Al6060 aluminum alloy	Al	Cr	Cu	Fe	Mg	Mn	Si	Ti	Zn
	97.9–99.3	0.05	0.1	0.1–0.3	0.35–0.5	0.1	0.3–0.6	0.1	0.15
Red copper alloy	Cu	Zn	Pb	Fe					
	84–86	14–16	0.05	0.05					

2 Experimental Setup

Figure 2 shows the designed and manufactured friction drilling machine with design details and specifications illustrated in the previous work [2]. The machine achieves a rotational speed range of 0–4200 rpm, and feed rate with a range of 0–218.182 mm/min. The used tools were offered by Flowdrill Company—Netherlands, with dimensions of tool diameter = 7.3 mm, center region angle = 90°, center region length = 0.94 mm, friction angle 30°, conical region length = 10.11 mm, and cylindrical region length = 8.89 mm. The tool material is tungsten carbide.

From previous researches, it was concluded that the shape of the A380 bushing was slightly improved by using very high rotational speed. Hence some trial experiments are conducted according to the manufactured machine performance, to prove previous researches and help in selecting the most suitable conditions. Table 2 illustrates the experimental matrix including the trial experiments. Noteworthy, experiment 1 of drilling A380 workpiece of 5 mm thickness is not completed. This is because this experiment is performed at the low rotational speed of 2000 rpm, so the produced heat due to friction is insufficient to completely perform the experiment, leading to tool-workpiece welding. Also, it is concluded from other trail experiments at different rotational speed, the minor change of bushing shape at higher rotational speed, as shown in Fig. 3. This occurs because, during bushing formation, much of the work-material is improperly flowed and does not form a bushing with the desired shape or added thickness to the hole for threading due to the occurrence of fracture.

Fig. 2 The manufactured friction drilling machine (a), machine control unit (b), Multi-component dynamometer (c), dynamometer data acquisition and amplifier (d), and laptop (e)

Table 2 The experimental matrix

Exp. no.	Workpiece material	Feed rate (mm/min)	Rotational speed (rpm)
Trail experiments			
1	A380 (5 mm)	100	2000
2			3000
3			3500
4			4000
5		160	4000
Material sandwich experiments			
6	316 stainless (1 mm)	120	4200
7	A380 alloy (5 mm) 316 stainless (1 mm)	160	
8	Al6060 alloy (1 mm)	120	
9	A380 alloy (5 mm) Al6060 alloy (1 mm)	160	
10	Red copper alloy (1 mm)	120	
11	A380 alloy (5 mm) Red copper alloy (1 mm)	160	

The AF is measured during drilling by a multi-component dynamometer (Kistler-type 9257B; measuring range −5 to 10 kN). It is observed that by increasing the rotational speed, the AF decreased. Figure 4 shows the obtained AF curve of the trail experiments 2 and 3.

3 Material Sandwich Experiments Implementation

Three materials; namely, 316 stainless steel, Al6060 aluminum alloy, red copper alloy are used with 1 mm thickness in which each of them is located on the upper and lower surfaces of A380 workpiece of 5 mm thickness, as illustrated in Fig. 5. These three materials are selected to compare their behavior in performing the idea of the functionally graded material. Also, each of them exhibits excellent properties that make them used in many important applications.

Fig. 3 The performed bushing of the trail experiments

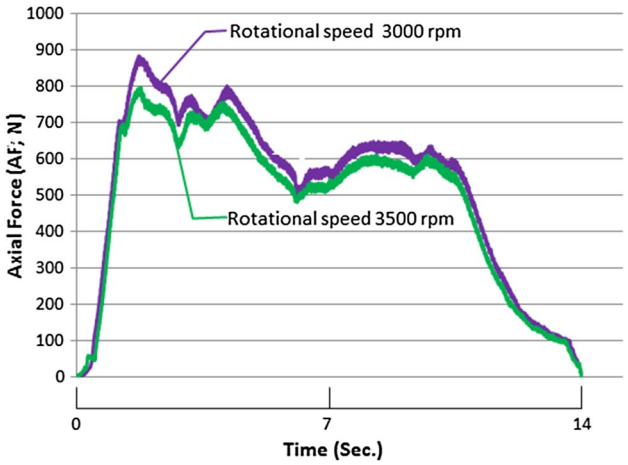

Fig. 4 The AF curves obtained while drilling A380 at 100 mm/min feed rate and different rotational speed

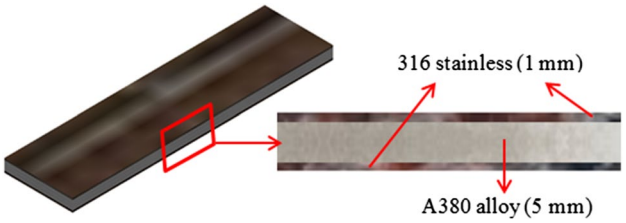

Fig. 5 Layout of A380 alloy workpiece and 316 stainless sheet metals

Austenitic grade 316 stainless steel contains 2–3% molybdenum, which improves the steel's resistance to pitting and crevice corrosion. This type of stainless is best suited for salt-water and marine applications, as well as highly acidic environments, needing the extra protection from chemical corrodents. Al6060 aluminum alloy exhibits very good corrosion resistance and weldability. Also, It has a very good anodizing response. It is commonly used for very complex cross-sections. Red copper alloy has excellent electrical and thermal conductivity, good strength, good formability and resistance to corrosion.

Since higher rotational speed is preferred, the maximum rotational speed of 4200 rpm obtained by the manufactured machine is used. Feed rate of 120 and 160 mm/min are applied to study its effect. The process parameter variations are studied according to material sandwiches experimental matrix illustrated in Table 2.

3.1 Axial Force

Figure 6 illustrates the obtained AF curves of experiments from 6 to 11. It is observed that by increasing the feed rate, the AF increases. The largest AF peak occurs with 316 stainless sandwich, while the smallest one occurs with Al6060

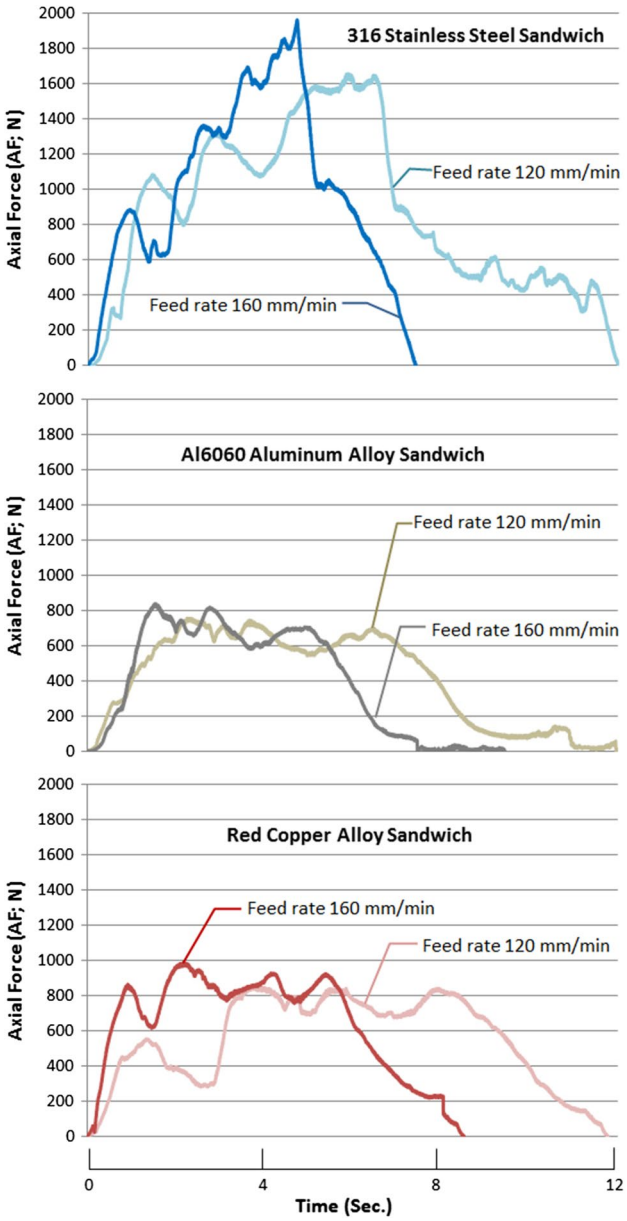

Fig. 6 The obtained AF curves of experiments from 6 to 11

alloy sandwich. This is because Al6060 alloy has the largest thermal conductivity, hence more flexibility of tool penetration due to heat generation from friction between the tool and workpiece.

3.2 Gap Area and Bushing Length

The gap can be measured according to two parameters; GT and GD. Figure 7 illustrates the GT, GD, and BL. The gap must be as small as possible because it may cause metal corrosion as a result of oxygen concentration occurring from an uneven

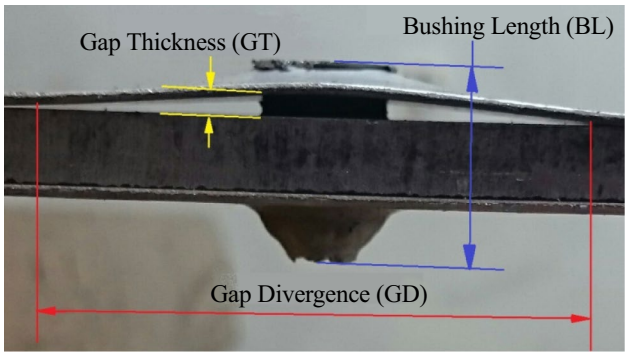

Fig. 7 Illustration of GT, GD and BL

metal surface exposed to air. Also, the BL must be as long as possible to allow longer high strength load bearing area.

Figure 8 shows the obtained bushing for all material sandwiches performed according to the experimental matrix. Table 3 illustrates the resultant measured GT, GD, and BL. From these results, lower feed rate achieves minimum GT and maximum BL, while minimum GD is obtained at larger feed rate for all material sandwiches. When the feed rate is low, more tool-workpiece contact time occurs, leading to more heat generation, so more BL during tool penetration. The largest BL obtained with 316 stainless sandwich, while the smallest one obtained with an Al6060 sandwich as it has the lowest elongation. The largest GT obtained with Al6060 alloy, while the smallest one obtained with 316 stainless. This is because Al6060 alloy has the largest thermal conductivity, so it takes less time to achieve plasticity state. Hence during penetration, the material that contacts the tool flows with it flexibly downward then upward, leading to more GT. The largest GD obtained with 316 stainless, while the smallest one obtained with Al6060 alloy. This is occurred due to more plasticity of Al6060 alloy than 316 stainless in the same time of contact, so more flexibility of Al6060 alloy leading to its bending during tool movement, hence lower GD.

4 Optimization by Fuzzy Logic Technique

Fuzzy logic technique is the proper tool for decision making of the best material sandwich according to the resultant AF peak, BL, GT, and GD. It can optimize the complicated multiple performance characteristics by mapping four inputs space to only one output space. Since the measured AF, BL, GT, and GD values are in different ranges, normalization to these values to the range of 0–1 must be performed before applying Fuzzy Logic technique. The normalized equation is expressed in Eq. 1 [9].

$$Np = (Xp - Xmin)/(Xmax - Xmin) \quad (1)$$

where Np is the normalized AF, BL, GT, or GD for every experiment number p, Xp is the AF, BL, GT, or GD for

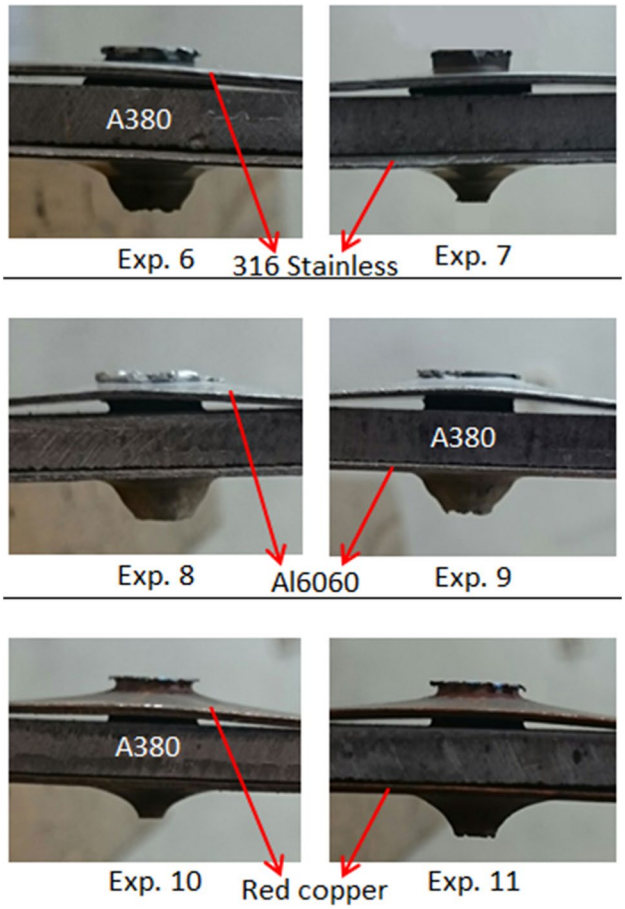

Fig. 8 The obtained bushing for all material sandwiches

experiment number p, $Xmax$ and $Xmin$ are the maximum and minimum values of the AF, BL, GT, or GD for all experiments. Table 4 shows the calculated normalized values.

MATLAB software is used to construct the inference model using Mamdani-type. The inputs for the inference system are the AF, BL, GT, and GD normalized values for every experiment and the output is named the multiple performance characteristic index (MPCI). Three

Table 3 The resultant GT, GD, and BL

	GT (mm)	GD (mm)	BL (mm)
316 stainless sandwich			
Exp. 6	0.35	38.35	14.39
Exp. 7	0.55	36.99	13.70
Al6060 alloy sandwich			
Exp. 8	1.29	35.72	13.58
Exp. 9	1.43	34.29	12.86
Red copper sandwich			
Exp. 10	0.58	37.15	14.29
Exp. 11	0.72	35.72	13.58

Table 4 The normalized AF, BL, GT, and GD

	N (AF)	*N* (BL)	*N* (GT)	*N* (GD)	MPCI
316 stainless sandwich					
Exp. 6	0.251	1.000	1.000	0.000	0.546
Exp. 7	0.000	0.549	0.815	0.335	0.436
Al6060 alloy sandwich					
Exp. 8	1.000	0.471	0.130	0.648	0.553
Exp. 9	0.932	0.000	0.000	1.000	0.492
Red copper sandwich					
Exp. 10	0.927	0.935	0.787	0.296	0.713
Exp. 11	0.807	0.471	0.657	0.648	0.639

Gaussian curve membership function fuzzy sets (i.e. low "L", medium "M", and high "H") are assigned to every input variable, while nine Gaussian curve membership function (i.e. very very low "VVL", very low "VL", low "L", low medium "LM", medium "M", medium-high "MH", high "H", very high "VH", and very very high "VVH") are assigned to the output variable. Eighty-one IF/THEN fuzzy rules are performed for mapping between the inputs and the output. The MPCI calculation based on centroid defuzzification method in the fuzzy inference model for experiment 10 as an example is demonstrated in Fig. 9a. The evaluated MPCI for all experiments are listed in Table 4 and plotted in Fig. 9b.

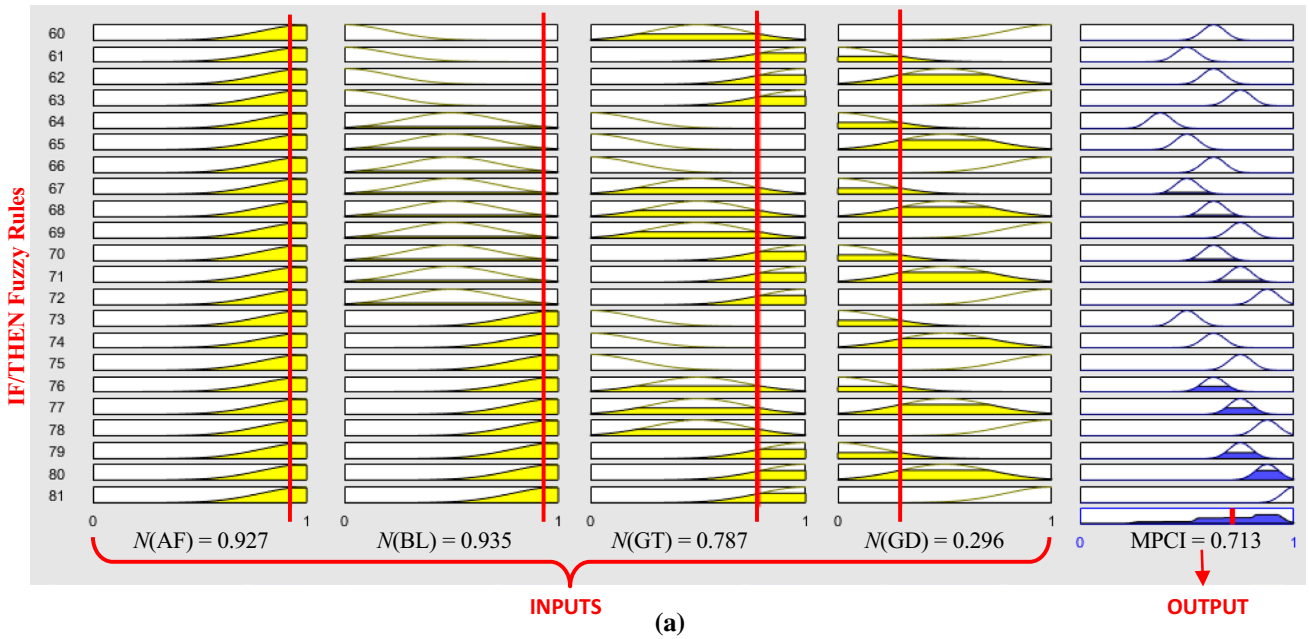

(a)

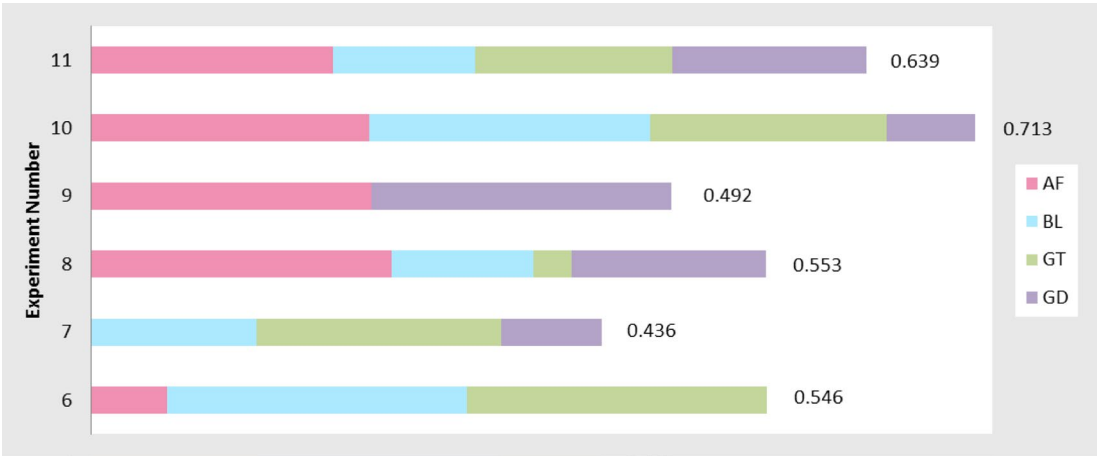

(b)

Fig. 9 **a** MPCI calculation based on centroid defuzzification method, **b** plotted MPCI

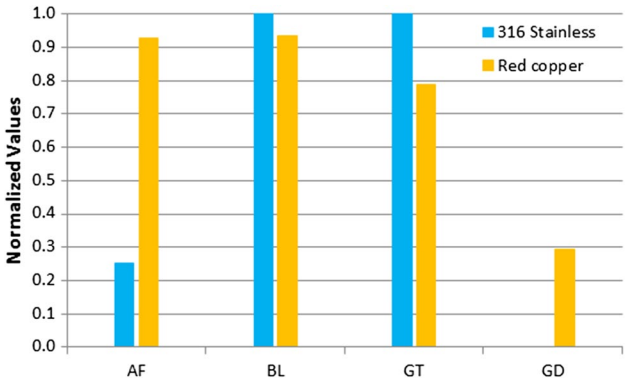

Fig. 10 The normalized values of 316 stainless and red copper alloy sandwiches at the optimal feed rate

The final results reveal that red copper sandwich exhibits the optimal MPCI. At lower feed rate the AF, BL, and GT are decreased with all material sandwiches, so lower feed rate is preferred. According to the three material sandwiches, Al6060 alloy sandwich achieves the optimal AF and GD but achieves the lowest BL and GT, which cannot make it desirable, as metal corrosion may occur and smaller strength load bearing area. Also, the outer surface of the bushing bottom is wrinkled. A comparison is performed between 316 stainless and red copper alloy sandwiches at 120 mm/min feed rate as they achieve close results according to the resultant BL and GT as demonstrated in Fig. 10. Based on the resultant AF and GD, red copper alloy sandwich is the best.

Hence the proposed idea achieves good results, especially with red copper sandwich. Figure 11 demonstrates the enhancement of the bushing; (a) shows the bushing top obtained with A380 alloy only, (b) shows the bushing top of A380 alloy obtained with Al6060 sandwich after removing the upper sheet of Al6060 alloy, (c) shows the bushing top of red copper sandwich, (d) shows the bushing bottom obtained with A380 alloy only, (e) shows the bushing bottom of A380 alloy obtained with red copper sandwich after removing the lower sheet of red copper alloy, (f) shows the wrinkled bushing bottom of Al6060 alloy sandwich.

5 Conclusions

This research has studied an idea for thermal friction drilling of cast aluminum alloy A380, to generate a cylindrical bushing without significant petal formation and radial fracture that are expected to be obtained. Three materials; namely, 316 stainless steel, Al6060 aluminum alloy, and red copper alloy are used in which each of them is located on the upper and lower surfaces of A380 workpiece, so achieving the idea of the functionally graded material. The process parameters are studied for reducing the axial force peak, gap thickness, gap divergence, and increasing the bushing length, with achieving a good bushing without petal formation and radial fracture. Experimental work is performed and concluded that lower feed rate achieves minimum axial force and gap thickness with maximum bushing length for all material sandwiches. An optimized decision making with the help of fuzzy logic techniques is performed. It reveals that the red copper sandwich exhibits the optimal multiple performance characteristic index based on axial

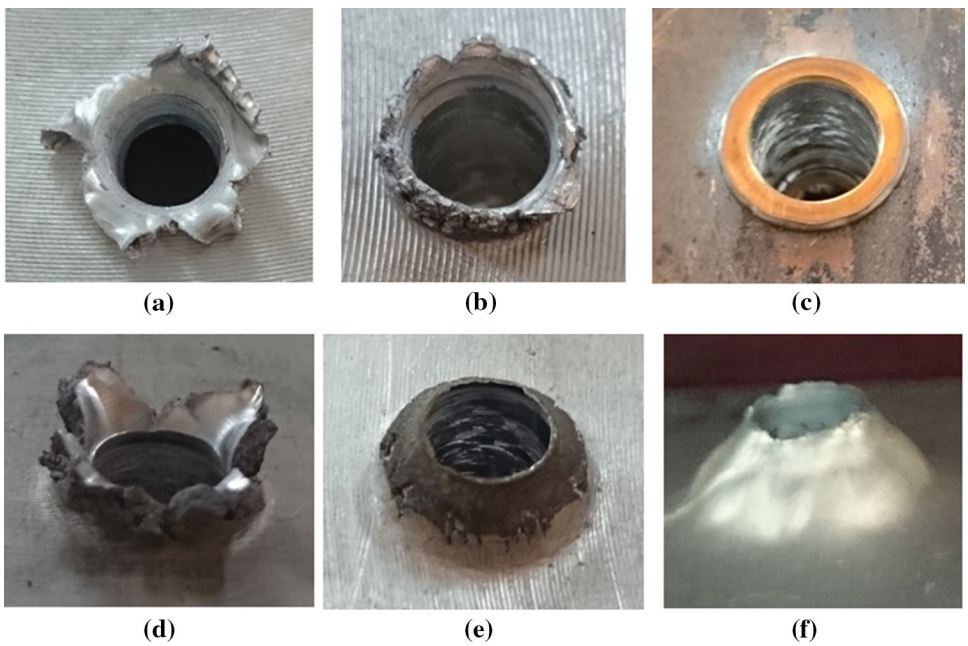

Fig. 11 **a** Bushing top of A380 alloy only, **b** bushing top of A380 alloy obtained with Al6060 sandwich, **c** bushing top of red copper sandwich, **d** bushing bottom of A380 alloy only, **e** bushing bottom of A380 alloy obtained with red copper sandwich, **f** wrinkled bushing bottom of Al6060 alloy sandwich

force, bushing length, gap thickness, and gap divergence. This research helps in decreasing the resultant axial force, so lower power consumption, hence lower machining cost. Longer bushing length is achieved, so more bearing area that can be threaded. Also, the gap is minimized leading to less metal corrosion that may be occurred as a result of oxygen concentration from an uneven metal surface exposed to air.

Acknowledgements The author would like to acknowledge Flowdrill Company—Netherlands for offering the needed tools. Also, she would like to acknowledge Shoman Company—Egypt for the valuable support in manufacturing the used thermal friction drilling machine.

References

1. Kaufman, J. G., & Rooy, E. L. (2004). *Aluminum alloy castings: Properties, processes, and applications*. Materials Park: ASM International.
2. El-Bahloul, S. A., El-Shourbagy, H. E., El-Bahloul, A. M., & El-Midany, T. T. (2018). Experimental and thermo-mechanical modeling optimization of thermal friction drilling for AISI 304 stainless steel. *CIRP Journal of Manufacturing Science and Technology, 20,* 84–92.
3. Miller, S. F., Tao, J., & Shih, A. J. (2006). Friction drilling of cast metals. *International Journal of Machine Tools and Manufacture, 46*(12–13), 1526–1535. https://doi.org/10.1016/j.ijmachtools.2005.09.003.
4. Lee, S., Chow, H., & Yan, B. (2007). Friction drilling of IN-713LC cast superalloy. *Materials and Manufacturing Processes, 22,* 893–897. https://doi.org/10.1080/10426910701451697.
5. Yang, L. D., Ku, W. L., Chow, H. M., Wang, D. A., & Lin, Y. C. (2012). Mar-M247, Haynes-230 and Inconel-718 study of machining characteristics for Ni-based superalloys on friction drilling. *Advanced Materials Research, 459,* 632–637. https://doi.org/10.4028/www.scientific.net/AMR.459.632.
6. Biermann, D., & Liu, Y. (2014). Innovative flow drilling on magnesium wrought alloy AZ31. *Procedia CIRP, 18,* 209–214. https://doi.org/10.1016/j.procir.2014.06.133.
7. Kaya, M. T., Aktas, A., Beylergil, B., & Akyildiz, H. K. (2014). An experimental study on friction drilling of ST12 steel. *Transactions of the Canadian Society for Mechanical Engineering, 38*(3), 319–329.
8. Urbikain, G., Perez, J. M., Lopez de Lacalle, L. N., & Andueza, A. (2016). Combination of friction drilling and form tapping processes on dissimilar materials for making nutless joints. *Proceedings of the Institution of Mechanical Engineers, Part B: Journal of Engineering Manufacture*. https://doi.org/10.1177/0954405416661002.
9. Nassar, K., Mahmod, W. E., Masria, A., Fath, H., & Nadaoka, K. (2018). Numerical simulation of shoreline responses in the vicinity of the western artificial inlet of the Bardawil Lagoon, Sinai Peninsula, Egypt. *Applied Ocean Research, 74,* 87–101.

Sara Ahmed El-Bahloul Lecturer of Production Engineering, Production and Mechanical Design Engineering Department, Faculty of Engineering, Mansoura University, Egypt. Her researches interested in production engineering, non-traditional machining, thermal friction drilling, design of experiments, optimization, fuzzy logic, and finite element analysis.